[CANCER RESEARCH 64, 8492–8495, December 1, 2004]

Advances in Brief

Bone Marrow Contribution to Tumor-Associated Myofibroblasts and Fibroblasts

Natalie C. Direkze,[1,2] Kairbaan Hodivala-Dilke,[1,3] Rosemary Jeffery,[1] Toby Hunt,[1] Richard Poulsom,[1] Dahmane Oukrif,[4] Malcolm R. Alison,[1,3] and Nicholas A. Wright[1,3]

[1]Cancer Research UK; [2]Imperial College London; [3]Barts and The London School of Medicine and Dentistry; and [4]University College, London, United Kingdom

Abstract

The role of myofibroblasts in tissue repair and fibrosis is well documented, but the source of these myofibroblasts is unclear. There is evidence of a circulating population of fibrocytes that can home to areas of injury and contribute to myofibroblast populations. Previously, we have shown that the bone marrow is a source of myofibroblasts for many tissues including the gut, lung, and kidney and that this phenomenon is exacerbated by injury. We now show that the bone marrow can contribute to myofibroblast and fibroblast populations in tumor stroma in a mouse model of pancreatic insulinoma. Mice transgenic for the rat insulin promoter II gene linked to the large-T antigen of SV40 (RIPTag) develop solid β-cell tumors of the pancreas. Approximately 25% of myofibroblasts in these pancreatic tumors were donor-derived, and these were concentrated toward the edge of the tumor. Thus, the development of tumor stroma is at least in part a systemic response that may ultimately yield methods of targeting new therapy.

Introduction

Myofibroblasts are ubiquitous cells with the features of both muscle cells and fibroblasts. They have significant roles in growth and differentiation as well as in inflammation, fibrosis and scarring (reviewed in ref. 1). Together, myofibroblasts and fibroblasts and the extracellular matrix proteins they produce are key components of the desmoplastic response to tumors (2). Both myofibroblasts and fibroblasts can be bone marrow-derived, and this phenomenon is augmented by injury (3). We now propose that bone marrow contributes to tumor stroma. We have investigated this using a mouse model of pancreatic insulinoma (4). The fate of bone marrow-derived cells was tracked by searching for male or green fluorescent protein (GFP)-positive cells in female GFP-negative recipients after whole-bone marrow transplantation.

Materials and Methods

Mice. All animal work was carried out under the British Home Office procedural and ethical guidelines. Recipient mice transgenic for the rat insulin promoter II gene linked to the large-T antigen of SV40 (RIPTag) develop solid β-cell tumors of the pancreas (4). Donor bone marrow was obtained from transgenic mice that carry GFP driven by a chicken β actin promoter [TgN(GFPU)5Nagy; Strain003115; The Jackson Laboratory, Bar Harbor, ME). Female RIPTag mice were divided into groups designed to receive sex- and GFP-mismatched bone marrow transplantation either before (8 weeks old) or after (10 weeks old) the expected development of tumors. The natural history of tumor development in these animals is for the mice to develop pancreatic dysplasia at approximately 9 weeks of age. The timings of the bone marrow transplant were therefore chosen as follows: (1) the transplant at 8 weeks to look at the capacity of bone marrow to contribute to myofibroblast and fibroblast populations in tumor stroma *per se*, and (2) the transplant at 10 weeks to assess whether this capacity still occurs after the development of the tumor, potentially a more clinically relevant situation. Wild-type female littermates also received sex- and GFP-mismatched bone marrow transplants at either 8 or 10 weeks to act as controls.

Transplant Protocol. Young adult female recipient mice (RIPTag) underwent whole-body γ irradiation with 12 Gray in a divided dose 3 hours apart to ablate their bone marrow. This was followed immediately by tail vein injection of 1 million male/GFP-positive whole-bone marrow cells as described previously (3). One male GFP-positive donor mouse supplied bone marrow for three recipient female mice. The mice were housed in sterile conditions. The animals were killed, and pancreata were harvested at approximately 8 weeks after bone marrow transplant on the development of signs of symptomatic tumors (hunching and seizures). The pancreata were fixed in neutral buffered formalin before being embedded in paraffin wax before analysis.

Immunohistochemistry. To identify donor cells in recipient mice, tissue sections were immunostained for GFP, or *in situ* hybridization for detection of the Y chromosome was performed. This was also performed in combination with various immunostains to identify cell types. Tissue sections were immunostained for α-smooth muscle actin (α SMA; mouse monoclonal Clone 1A4, A-2547; Sigma, Poole, United Kingdom), vimentin (Vim; Clone 3B4; M7020; Dako, Buckinghamshire, United Kingdom), insulin (rabbit polyclonal; 11187; ICN Biomedicals, Ltd., Basingstoke, United Kingdom), F4/80 (rat antimouse; MCA497B; Serotec, Ltd., Oxford, United Kingdom), CD45 (rat antimouse; 550539; Becton Dickinson, Oxford, United Kingdom), GFAP (rabbit polyclonal; Z0334; Dako), CD34 (rat antimouse; CL8927AP; Accurate Chemical, Westbury, NY) and SV40 large T antigen (KT3; Cancer Research UK). Tissue sections were immunostained as described previously (3) with modifications for certain antibodies; extra antigen retrieval was required in the form of microwaving for 10 minutes in trisodium citrate buffer at pH 6 (insulin/GFP), or treatment with trypsin at pH 7.8 for 15 minutes (CD34 and CD45). After the three-step immunodetection protocol, sections were washed in PBS and Vector Red substrate (SK 5100; Vector Laboratories, Peterborough, United Kingdom) or 3,3′-diaminobenzidine in solution were applied to visualize. Sections were again washed in PBS before the *in situ* hybridization protocol.

***In situ* Hybridization.** *In situ* hybridization to visualize the Y chromosome was conducted as described previously (3). In brief, after immunohistochemistry, sections were permeablized and digested with pepsin. The protease was quenched, and sections were post-fixed and dehydrated through graded alcohols before air drying. A fluorescein isothiocyanate-labeled Y-chromosome paint (Star-FISH; Cambio, Cambridge, United Kingdom) was used in the supplier's hybridization mix. The probe mixture was added to the sections, sealed under glass with rubber cement, heated to 60°C for 10 minutes, and incubated overnight at 37°C. Post-hybridization washes were then completed as described previously with standard sodium citrate washes of decreasing stringency. Slides to be viewed by fluorescent microscopy (insulin/SV40 large T antigen) were then washed in PBS before mounting in Vectashield with 4′,6-diamidino-2-phenylindole (Vector Laboratories). All slides to be viewed indirectly were then washed with PBS and incubated with 1:250 peroxidase-conjugated antifluorescein antibody (150 U/mL; Boehringer Mannheim, Mannheim, Germany) for 60 minutes at room temperature. These slides were developed in 3,3′-diaminobenzidine (0.005 g in 10 mL of PBS) plus hydrogen peroxide (20 μL), counterstained with hematoxylin and mounted in dibutylpthalate xylene (DPX).

Counting and Statistics. To assess the number of bone marrow-derived myofibroblasts contributing to the tumor stroma, the numbers of bone marrow-

Received 5/17/04; revised 8/27/04; accepted 10/15/04.

Grant support: Cancer Research United Kingdom.

The costs of publication of this article were defrayed in part by the payment of page charges. This article must therefore be hereby marked *advertisement* in accordance with 18 U.S.C. Section 1734 solely to indicate this fact.

Requests for reprints: Natalie C. Direkze, Histopathology Unit, Cancer Research United Kingdom London Research Institute, 44 Lincoln's Inn Fields, London, WC2A 3PX, United Kingdom. Phone: 44-20-7269-3245; Fax: 44-20-7269-3491; E-mail: natalie.direkze@cancer.org.uk.

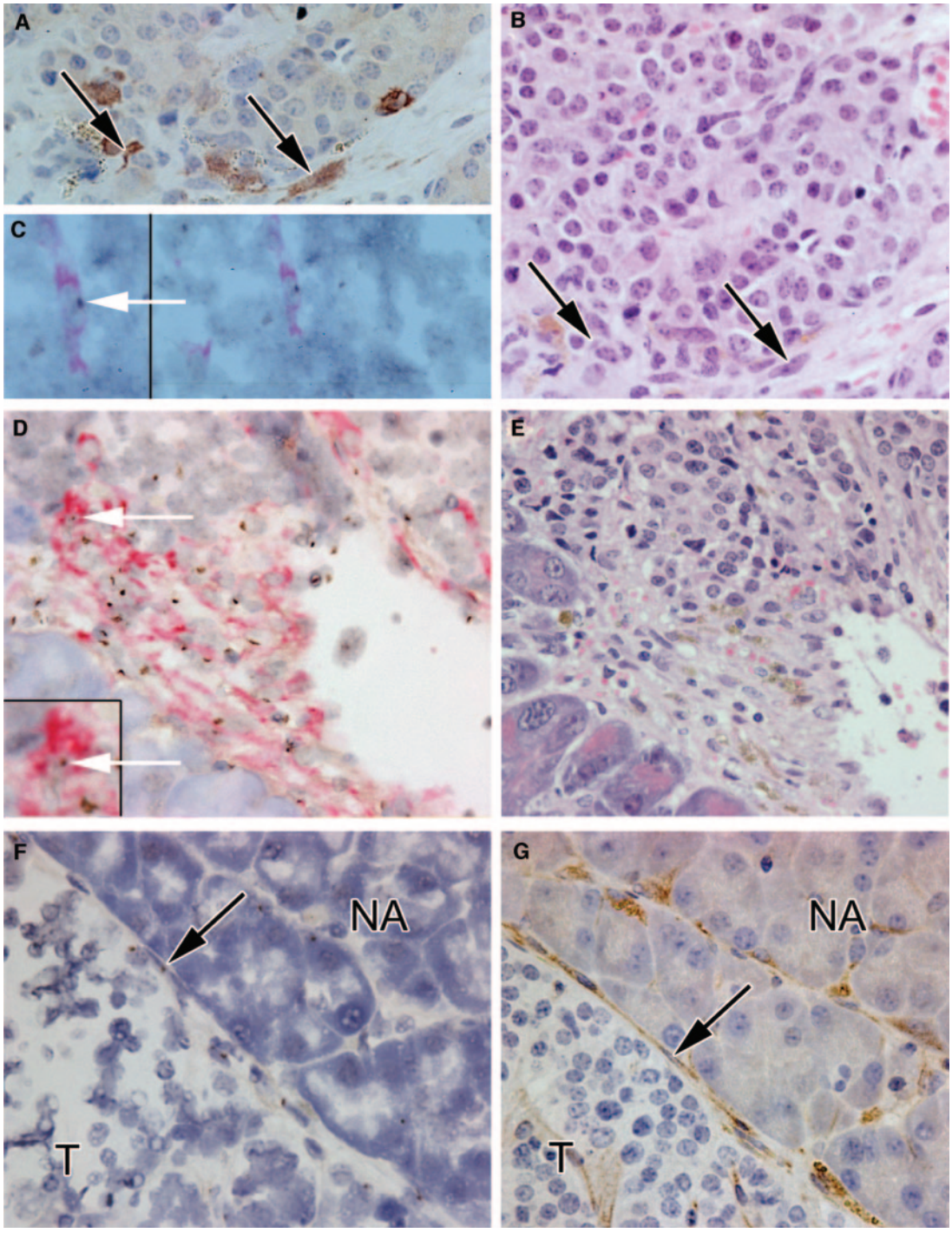

Fig. 1. To show donor-derived cells with differing immunophenotypes. Female mice have been transplanted with male GFP-positive whole bone marrow. Donor-derived cells are identified by the presence of a Y chromosome (*brown dot*, *in situ* hybridization) or GFP positivity. *A*, immunohistochemistry for GFP (*brown stain*; ×40 magnification). Numerous donor-derived cells, including some with a fibroblastic morphology. *B*, the same section stained with hematoxylin and eosin to illustrate the morphology of these cells and local tumor cells. *C*, immunostain for CD34 (*red*) and *in situ* hybridization for Y chromosome (*brown dot*; ×40); donor-derived CD34-positive cell magnified in *inset* (×100). *D*, immunostain for α SMA (*red*) and *in situ* hybridization for the Y chromosome (*brown dot*; ×20). Numerous male cells are seen at the junction between the tumor and surrounding pancreas; one of these donor-derived myofibroblasts is enlarged (×60; *white arrow*, *inset*). *E*, hematoxylin and eosin (×20) to show similar area to that in *D*, outlines morphology of tumor border. *F*, section to show tumor edge immunostained for α SMA (*red*) and *in situ* hybridization for the Y chromosome (*brown dot*; ×40). An α SMA-negative, donor-derived (Y-positive) spindle-shaped cell labeled with a *black arrow* (*NA*, normal acini; *T*, tumor). *G*. In the serial section to this immunostained for vimentin (*brown stain*), this cell is vimentin positive (*black arrow*), a donor-derived fibroblast (×40).

derived myofibroblasts within 1 high-power field (×40 objective) of the tumor margin were counted as a fraction of the total number of myofibroblasts in the same area (>1900 cells were counted) in the tumor-bearing mice. In addition, the number of bone marrow-derived myofibroblasts were counted in the center of the tumor (more than 1 high-power field away from the tumor margin) again as a fraction of the total number of myofibroblasts within the same area. Bone marrow-derived myofibroblasts in wild-type littermate pancreas was also counted as a proportion of the total number of myofibroblasts. The means of each group were compared using a two-tailed *t* test.

Results

Myofibroblasts were identified by their morphology and α SMA expression. Fibroblasts were identified by their morphology (on

Table 1 *Quantification of tumor-associated donor derived myofibroblasts*

	Y-positive myofibroblasts [mean % ± SD (total HPFs scored)]			
	BMTx at 8 wks of age	BMTx at 10 wks of age	Control	*P*
Tumor edge	29 ± 9% (406)	22 ± 5% (310)	10 ± 5% (1,746)	Tumor edge *vs.* control, BMTx at 8 weeks of age = 0.0019* Tumor edge *vs.* control, BMTx at 10 weeks of age = 0.004*
Tumor middle	19 ± 9% (346)	14 ± 5% (648)	10 ± 5% (1,746)	Not significant
Tumor total	29 ± 13% (752)	20 ± 4% (958)	10 ± 5% (1,746)	Tumor total *vs.* control, BMTx at 8 weeks of age = 0.0088* Tumor total *vs.* control, BMTx at 10 weeks of age = 0.0063*
Tumor edge (BMTx groups pooled)	25 ± 8%		10 ± 5%	Tumor edge *vs.* control = 0.0009*
Tumor middle (BMTx groups pooled)	17 ± 7%		10 ± 5%	Tumor edge *versus* middle = 0.0495*

NOTE. There was a significantly higher proportion of bone marrow-derived myofibroblasts at the margin of the tumor (the site of the desmoplastic reaction) in comparison with control tissue and the center of the tumor. We did not find a significant difference in the level of engraftment when the transplant occurred either before or after the anticipated development of pancreatic tumors. This time course was initially designed to represent a more clinically relevant situation, *i.e.*, bone marrow transplant after tumor development. However, because there was no significant difference between levels of engraftment between the groups, data from these two groups were pooled in the final analysis as indicated in the table. Group size: 8 weeks old, $n = 4$; 10 weeks old, $n = 4$; control, $n = 6$.

Abbreviations: BMTx, bone marrow transplant; HPF, high-power field.

* Statistically significant *P* values.

hematoxylin and eosin) and vimentin expression. Cells were identified as being donor-derived either by the presence of a Y chromosome in a female mouse or by their GFP positivity (Fig. 1*A* and *B*)

Overall, approximately 25% of myofibroblasts were found to be bone marrow-derived in pancreatic tumors (Table 1). These tended to be concentrated within one high-power field of the tumor edge. Approximately 25% of myofibroblasts were bone marrow-derived at the edge of the tumor as compared with 17% in the center ($P < 0.05$; Fig. 1*D*).

We did not see a significant difference between the level of engraftment in those mice transplanted before the anticipated development of tumors (transplant at 8 weeks; mean engraftment 29 ± 13%; $n = 4$) and those transplanted at 10 weeks, which was after the anticipated development of tumors (mean engraftment 20% ± 4%; $n = 4$). Very occasional CD34-positive donor-derived cells were seen (Fig. 1*C*).

The tumors expressed insulin, and occasional insulin-positive cells were donor-derived (Fig. 2*A*). We also found evidence of SV40 large T antigen-positive cells that were also Y positive and therefore suggestive of cell fusion (Fig. 2*B*).

There were donor-derived fibroblasts expressing vimentin (Fig. 1*G*) but not α SMA (Fig. 1*F*). In keeping with hematopoietic reconstitution, CD45- and F4/80-positive donor-derived cells were seen particularly at the tumor margin (not shown).

Discussion

We have shown that the bone marrow contributes to myofibroblast and fibroblast populations in a mouse model of pancreatic insulinoma. Additionally, we have shown in our mouse model that bone marrow can contribute to insulin-producing cell types within the insulinomas and also that there are cells that display phenotypic characteristics of both the donor and the recipient (SV40 and Y).

In the development of tumors, the interaction between the tumor and the host is often characterized by a desmoplastic reaction. The role of the desmoplastic response to tumors is not completely understood although a cancer-induced change in the stroma may contribute to cancer invasion (5).

In normal circumstances, the interaction between normal epithelium and normal stroma helps to maintain tissue integrity. However, in cancer, the interaction between cancer cells and the surrounding stroma via signals such as transforming growth factor β and platelet-derived growth factor results in the formation of an abnormal stroma, the disruption of tissue integrity, and hence invasion and ultimately metastasis (reviewed in ref. 2). Potential

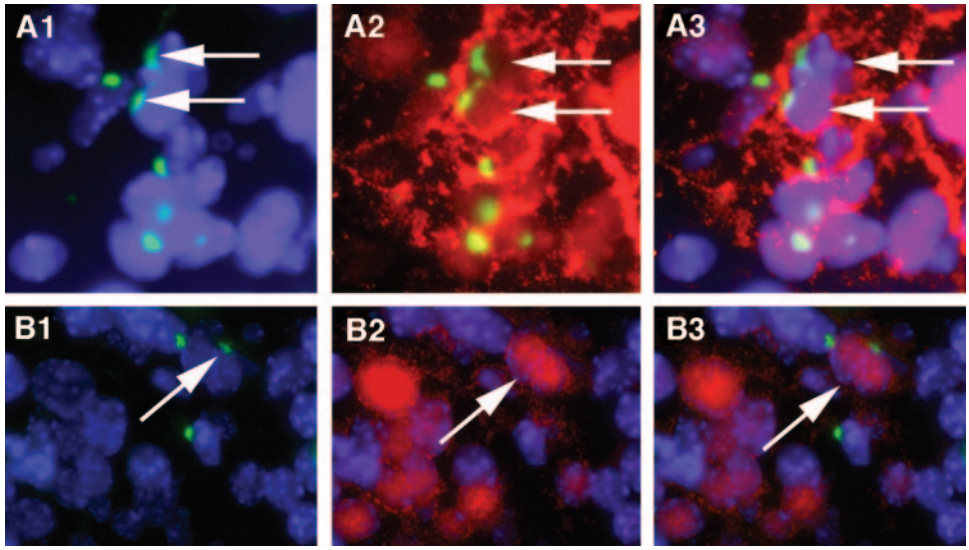

Fig. 2. To show donor-derived cells with differing immunophenotypes directly. *A1*, section from a tumor in a RIPTag mouse after male GFP whole-bone marrow transplant (×63). Donor-derived cells are visualized by *in situ* hybridization for the Y chromosome (*green dot*), two of which are labeled with *white arrows*. *A2*, the same section again illustrating the donor-derived cells (*green dots*) combined with immunohistochemistry for insulin (*red*). *A3*, the merged image of the donor-derived insulin-positive cells with the nuclei outlined with 4′,6-diamidino-2-phenylindole (*blue*); again, two of these cells are indicated with *white arrows*. *B1*, section from a tumor in a female RIPTag mouse after male/GFP-positive bone marrow transplant (×63). Donor-derived cells are visualized by *in situ* hybridization for the Y chromosome (*green dot*), one of which is indicated with a *white arrow*. *B2*, the same section immunostained for SV40 T antigen (*red*), which is expressed in tumor cells in this model. *B3*, the merged image of *B1* and *B2*. Although there are SV40 T-positive cells that are not Y positive in this plate, the *arrow* indicates a cell that is both SV40 T antigen positive and Y positive.

key participants in the development of this stroma are circulating fibroblasts (6), and there is evidence that given the appropriate environment, modulation of fibroblast differentiation toward a myofibroblast phenotype can occur (reviewed in ref. 7). The full role of these myofibroblasts in cancer is not known. There is some evidence that they may shield cancer cells from the immune response and therefore increase their capacity to invade (8). On the other hand, patients with encapsulated hepatocellular carcinomas have improved survival in comparison with those with nonencapsulated tumors (9). Also, the presence of myofibroblasts around the most aggressive tumors is associated with an absence of immune and inflammatory cells [leukocytes being implicated in some studies with assistance in tumor invasion (10)]. "Myofibroblast-like" cells (α SMA-positive) are the source of capsular collagen in human hepatocellular carcinomas (11, 12). Furthermore, transforming growth factor β1 produced by nontumor cells at the tumor interface may perpetuate the myofibroblastic phenotype and result in the formation of the tumor capsule (12). In rectal adenocarcinoma, the type of stroma is associated with the prognosis; those with an immature or myxoid stromal type have a higher proportion of myofibroblasts and have a worse prognosis (13).

The source of myofibroblasts is not yet fully defined. Epithelial cells may also act as precursors for myofibroblasts, so-called epithelial-mesenchymal transitions (reviewed in ref. 14). In this study, we have now shown that bone marrow can contribute to tumor stroma. Bone marrow-derived cells were found both within and around the pancreatic tumors that developed in the RIPTag mice. Although α SMA-positive, donor-derived cells were found throughout the tumors, significantly higher numbers were found at the tumor margins, the predominant site of the desmoplastic reaction (Fig. 1*D*).

As expected, CD34-positive donor bone marrow-derived cells were seen (see Fig. 1*C*). CD34-positive fibrocytes are important cells in various pathologies and tend to be depleted in malignant lesions as compared with benign ones (15, 16). In the pancreas, CD34-positive stromal cells are found to be more characteristic of chronic inflammatory lesions but do exist in neoplastic lesions. In a study of human islet cell tumors, myofibroblasts were present in tumor stroma in the center of the tumors, whereas myofibroblasts and CD34-positive stromal cells were found in the tumor capsule (17).

The islet tumors of the pancreas produce insulin. Ianus *et al.* (18) have provided clear evidence of bone marrow-derived insulin-producing cells being generated without cell fusion. We also found occasional donor-derived insulin-producing cells in the tumors (Fig. 2*A*). To assess whether this finding was due to fusion of bone marrow-derived cells with tumor cells or transdifferentiation, we looked for SV40 large T antigen-positive cells that were also Y positive. SV40 large T antigen is expressed by insulin-producing cells of the RIPTag mouse. By finding SV40 large T antigen-positive (recipient marker) cells that were also Y positive (donor marker), we provide evidence of cell fusion between the tumor cells and the donor bone marrow-derived cells. In a similar vein, Grompe et al. (19) showed fusion between female bone marrow donor cells and recipient fumarylacetoacetate-deficient hepatocytes through observation of a donor trait (fumarylacetoacetate positivity) combined with a recipient trait (Y chromosome) in the same cell.

In summary, we have demonstrated that the bone marrow can contribute to the tumor microenvironment in a murine model of pancreatic cancer. We have shown that there is significant contribution to myofibroblast populations within the tumor and that this is more marked at the tumor margin. Additionally, we have also demonstrated that bone marrow-derived cells may also fuse with insulin-producing cells within tumors in this model. Although these findings suggest that the development of tumor stroma is a less localized phenomenon that previously thought, the question remains as to whether the bone marrow contribution to tumor stroma is part of a host defense mechanism or a reflection of cell recruitment by tumors.

Acknowledgments

We thank D. Hanahan for providing the RIPTag mice.

References

1. Powell DW, Mifflin RC, Valentich JD, Crowe SE, Saada JI, West AB. Myofibroblasts: I. Paracrine cells important in health and disease. Am J Physiol 1999;277: C1–9.
2. De Wever O, Mareel M. Role of tissue stroma in cancer cell invasion. J Pathol 2003;200:429–47.
3. Direkze NC, Forbes SJ, Brittan M, et al. Multiple organ engraftment by bone-marrow-derived myofibroblasts and fibroblasts in bone-marrow-transplanted mice. Stem Cells 2003;21:514–20.
4. Hanahan D. Heritable formation of pancreatic beta-cell tumours in transgenic mice expressing recombinant insulin/simian virus 40 oncogenes. Nature 1985; 315:115–22.
5. Liotta LA, Kohn EC. The microenvironment of the tumour-host interface. Nature (Lond) 2001;411:375–9.
6. Abe R, Donnelly SC, Peng T, Bucala R, Metz CN. Peripheral blood fibrocytes: differentiation pathway and migration to wound sites. J Immunol 2001;166:7556–62.
7. Gabbiani G. The myofibroblast in wound healing and fibrocontractive diseases. J Pathol 2003;200:500–3.
8. Lieubeau B, Heymann MF, Henry F, Barbieux I, Meflah K, Gregoire M. Immunomodulatory effects of tumor-associated fibroblasts in colorectal-tumor development. Int J Cancer 1999;81:629–36.
9. Ng IO, Lai EC, Ng MM, Fan ST. Tumor encapsulation in hepatocellular carcinoma: a pathologic study of 189 cases. Cancer (Phila) 1992;70:45–9.
10. Opdenakker G, Van Damme J. Chemotactic factors, passive invasion and metastasis of cancer cells. Immunol Today 1992;13:463–4.
11. Ooi LP, Crawford DH, Gotley DC, et al. Evidence that "myofibroblast-like" cells are the cellular source of capsular collagen in hepatocellular carcinoma. J Hepatol 1997;26:798–807.
12. Bridle KR, Crawford DH, Powell LW, Ramm GA. Role of myofibroblasts in tumour encapsulation of hepatocellular carcinoma in haemochromatosis. Liver 2001;21: 96–104.
13. Ueno H, Jones AM, Wilkinson KH, Jass JR, Talbot IC. Histological categorisation of fibrotic cancer stroma in advanced rectal cancer. Gut 2004;53:581–6.
14. Kalluri R, Neilson EG. Epithelial-mesenchymal transition and its implications for fibrosis. J Clin Investig 2003;112:1776–84.
15. Nakayama H, Enzan H, Miyazaki E, Kuroda N, Naruse K, Hiroi M. Differential expression of CD34 in normal colorectal tissue, peritumoral inflammatory tissue, and tumour stroma. J Clin Pathol 2000;53:626–9.
16. Chauhan H, Abraham A, Phillips JR, Pringle JH, Walker RA, Jones JL. There is more than one kind of myofibroblast: analysis of CD34 expression in benign, in situ, and invasive breast lesions. J Clin Pathol 2003;56:271–6.
17. Kuroda N, Toi M, Nakayama H, et al. The distribution and role of myofibroblasts and CD34-positive stromal cells in normal pancreas and various pancreatic lesions. Histol Histopathol 2004;19:59–67.
18. Ianus A, Holz GG, Theise ND, Hussain MA. In vivo derivation of glucose-competent pancreatic endocrine cells from bone marrow without evidence of cell fusion. J Clin Investig 2003;111:843–50.
19. Wang X, Willenbring H, Akkari Y, et al. Cell fusion is the principal source of bone-marrow-derived hepatocytes. Nature (Lond) 2003;422:897–901.